Acta Geologica Sinica (English Edition), 2021, 95(2): 319–332

A Juvenile Specimen of Sauropodomorpha from the Lower Jurassic of China and a Brief Review of the Lufeng Sauropodomorph Fauna

Claire PEYRE DE FABRÈGUES[1, *], BI Shundong[1, 2], AI Tianyu[3] and XU Xing[4]

[1] *Centre for Vertebrate Evolutionary Biology, Institute of Palaeontology, Yunnan University, Kunming 650091, China*
[2] *Department of Biology, Indiana University of Pennsylvania, Indiana, PA 15705, USA*
[3] *Independent Researcher, Kunming 650091, China*
[4] *Key Laboratory of Evolutionary Systematics of Vertebrates, Institute of Vertebrate Paleontology & Paleoanthropology, Chinese Academy of Sciences, Beijing 100044, China*

Abstract: An incomplete dinosaur skeleton, including a partial skull, recently discovered from the Lower Jurassic Lufeng Formation of Yunnan, China, is here reported. Apart from its small size, little anatomical evidence supports, a priori, the non-adult status of this new sauropodomorph specimen but osteohistological analyses suggest that it is a fast-growing juvenile. This specimen represents only the second occurrence of a juvenile non-sauropodan sauropodomorph in the Lufeng Basin. The anatomy of the new specimen does not match that of other Lower Jurassic immature specimens; although cranial material is preserved, it does not display the diagnostic characters of early sauropodomorphs from the same horizon, namely *Lufengosaurus*, *Yizhousaurus* and *Yunnanosaurus*. Our phylogenetic analysis places the new specimen in a position relatively distant from other Chinese sauropodomorphs, and corroborates the anatomical evidence showing it is not referable to any known species already excavated in Yunnan. This result is interpreted with caution considering that ontogeny affects phylogenetic reconstruction. A thorough comparison with adult forms, taking into account ontogeny-related characters, suggests that this Lufeng juvenile might represent a previously unknown species of early sauropodomorph.

Key words: Sauropodomorpha, juvenile, faunal review, Jurassic, Lufeng, Yunnan province

Citation: Peyre de Fabrègues et al., 2021. A Juvenile Specimen of Sauropodomorpha from the Lower Jurassic of China and a Brief Review of the Lufeng Sauropodomorph Fauna. Acta Geologica Sinica (English Edition), 95(2): 319–332. DOI: 10.1111/1755-6724.14707

1 Introduction

It was not until the 1970s that paleontologists came to realize that many dinosaur specimens represent immature individuals. Since then, hundreds of them have been identified and studied. Among sauropodomorph dinosaurs, one of the earliest reports of a young sauropod was made by Marsh (1883) and the skeleton was later assigned to *Camarasaurus* (Carpenter and McIntosh, 1994). Among non-sauropodan sauropodomorphs, some 20 juveniles have been published throughout the world, not counting embryos. A few specimens are still indeterminate to date, but most of them have been assigned to new or already existing genera. Non-sauropodan sauropodomorph juveniles attributed to six different genera, as well as one indeterminate specimen, were reported from Upper Triassic deposits: *Efraasia* (Galton and Bakker, 1985), *Thecodontosaurus* (Benton et al., 2000), *Euskelosaurus* (Durand, 2001), *Mussaurus* (Pol and Powell, 2007; Cerda et al., 2014), *Pantydraco* (Galton et al., 2007; Galton and Kermack, 2010), *Plateosaurus* (Hofmann and Sander, 2014), and MMACR-PV-028-T (Pretto et al., 2016). Similarly, five non-sauropodan sauropodomorph juveniles were reported from Lower Jurassic deposits: *Arcusaurus* (Yates et al., 2011), *Ignavusaurus* (Knoll, 2010), *Lufengosaurus* (Sekiya and Dong, 2010), *Massospondylus* (Sues et al., 2004), and *Yunnanosaurus* (Sekiya et al., 2014), as well as two indeterminate specimens (Young, 1982; Evans and Milner, 1989; Sereno, 1991). Juvenile remains attributed to *Ammosaurus*, *Riojasaurus* and *Ruehleia* have also been mentioned, but never properly described (Galton and Upchurch, 2004).

The first description of a juvenile non-sauropodan sauropodomorph in China dates back to the 1980s (Young, 1982). Since then, many other specimens, both adult and non-adult, have been recovered in China, particularly from the Lufeng Formation (Fm., lower part of the Lufeng Group) of Yunnan Province. Nearly all the species recovered in Yunnan were first reported from the Lufeng Fm., currently the richest fossil-bearing Mesozoic unit in the province (Luo and Wu, 1994; Mao et al., 2019). Nevertheless, most retrieved specimens have not yet been studied, thus preventing observation of possible growth stages. Accordingly, few non-adult specimens from Yunnan have been reported in the literature: most information on early ontogenetic stages of Chinese taxa is

* Corresponding author. E-mail: claire.pdf@gmail.com

based upon three patchy specimens (Young, 1982; Evans and Milner, 1989; Sekiya and Dong, 2010), and a single more complete one (Sekiya et al., 2014).

In 2018, a new specimen identified here as a juvenile non-sauropodan sauropodomorph was excavated from the Lufeng Fm. Those same strata have yielded several specimens of *Lufengosaurus* (Young, 1941), *Yunnanosaurus* (Young, 1942), as well as *Yizhousaurus* (Zhang et al., 2018). In this paper, we hereby review the faunal sauropodomorph diversity of the so-called "Lufeng Group" (Sun et al., 1985; Fang et al., 2000), before describing the new specimen and discussing its age and taxonomy.

2 Geological Background and Faunal Content

2.1 Geology of Lufeng Basin

The juvenile specimen reported herein was unearthed near Dahuangtian Village, Lufeng County, Yunnan Province, China (Fig. 1). The first dinosaur from the Lufeng Fm. of Dahuangtian Village was reported by Young (1948). Dahuangtian is known to be one of the major fossil localities in the Lufeng Fm., along with Dawa, from where embryos, potentially referable to *Lufengosaurus*, were recently described (Reisz et al., 2013), and a few other locations (Luo and Wu, 1994; Kielan-Jaworowska et al., 2004). These localities are located within the Early to Middle Jurassic of the Lufeng Basin, which only encompasses a fraction of the historical Mesozoic 'Red Beds' outcrops, also called the 'Lufeng Group' (Fig. 1). Some other sedimentary basins containing the same sediments include the Chuxiong Basin, located west of the Lufeng Basin, and the Fumin Basin, to the east.

The Mesozoic 'Red Beds', exposed in the center of the province, represent one of the major dinosaur-bearing rock units of the Lower Jurassic to Lower Cretaceous succession of southwestern China (Fang et al., 2008). The sediments are mainly mudstones and show a progression from shallow lacustrine to dryer paleoenvironments (Luo and Wu, 1994, 1995; Racey and Goodall, 2009, fig. 2).

The base of the unit, the Lufeng Fm., is in conformity with the underlying Proterozoic Etouchang Fm. The top of the Lufeng Fm. unconformably underlies the Middle Jurassic Chuanjie Fm., formerly known as the "Upper Lufeng Fm." (Fang et al., 2000). The Lufeng Fm. is 272 m thick, and composed of sediments of various grain sizes, mostly deep red and dark purple-red mudstones interbedded with thinly laminated siltstones (Zhang and Li, 1999; Fang et al., 2000). The deposition of the Lufeng Fm. is interpreted as the transition from a shallow lacustrine area to a plain with alluvial soils (Luo and Wu, 1995). These sediments have been dated as Early Jurassic (Luo and Wu, 1994), with further evidence supporting this dating provided by the Lufeng vertebrate assemblages, as well as those of its lateral equivalent, the Fengjiahe Fm. (Dong, 1992; Luo and Wu, 1994).

The Lufeng Fm. is subdivided into two members: the Shawan Member, originally called "Dull Purplish Beds" of the "Lower Lufeng Fm.", is in conformity with the overlying Zhangjia'ao Member, originally called "Dark Red Beds" of the "Lower Lufeng Fm." (Young, 1951;

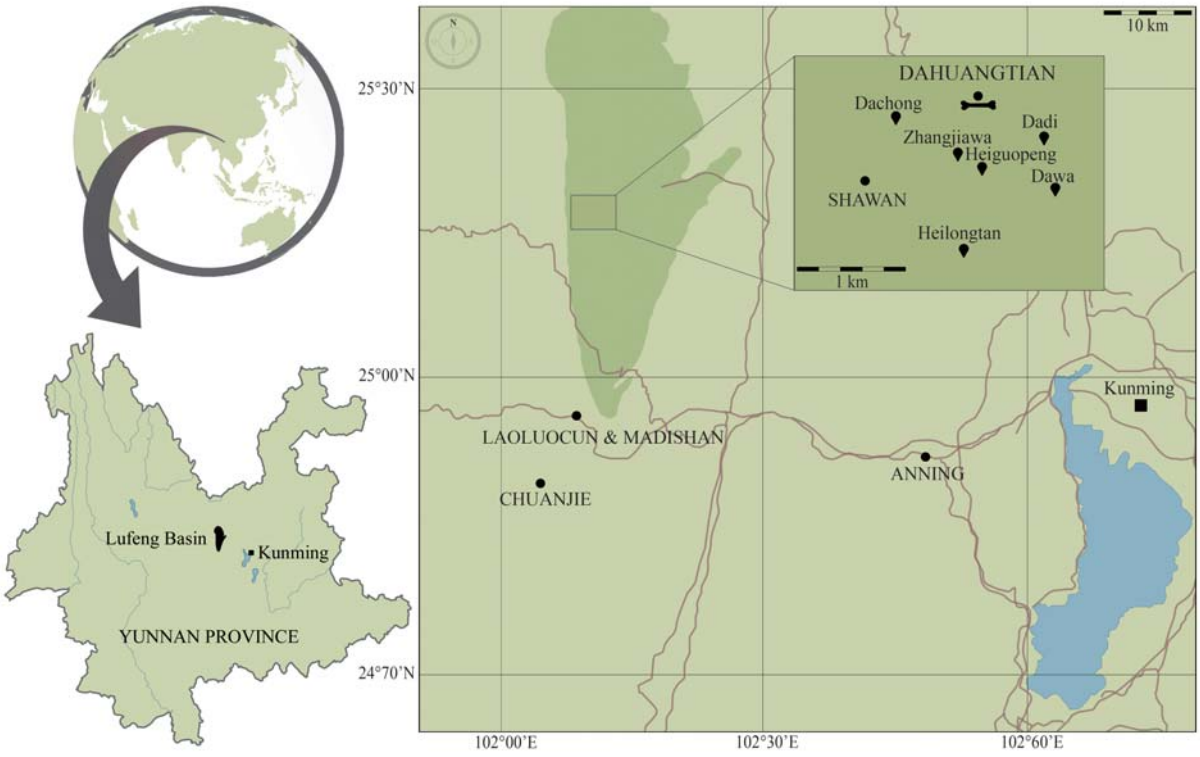

Fig. 1. Geographic map showing locality of new fossil CVEB22001 and its surroundings.
Towns and villages where type sections of the "Lufeng Group" were originally established indicated by circles; major localities of the Lufeng Fm. indicated by pins. The darker green shape shows the Lufeng Basin (modified from Luo and Wu, 1994). Capitalized localities contain type sections.

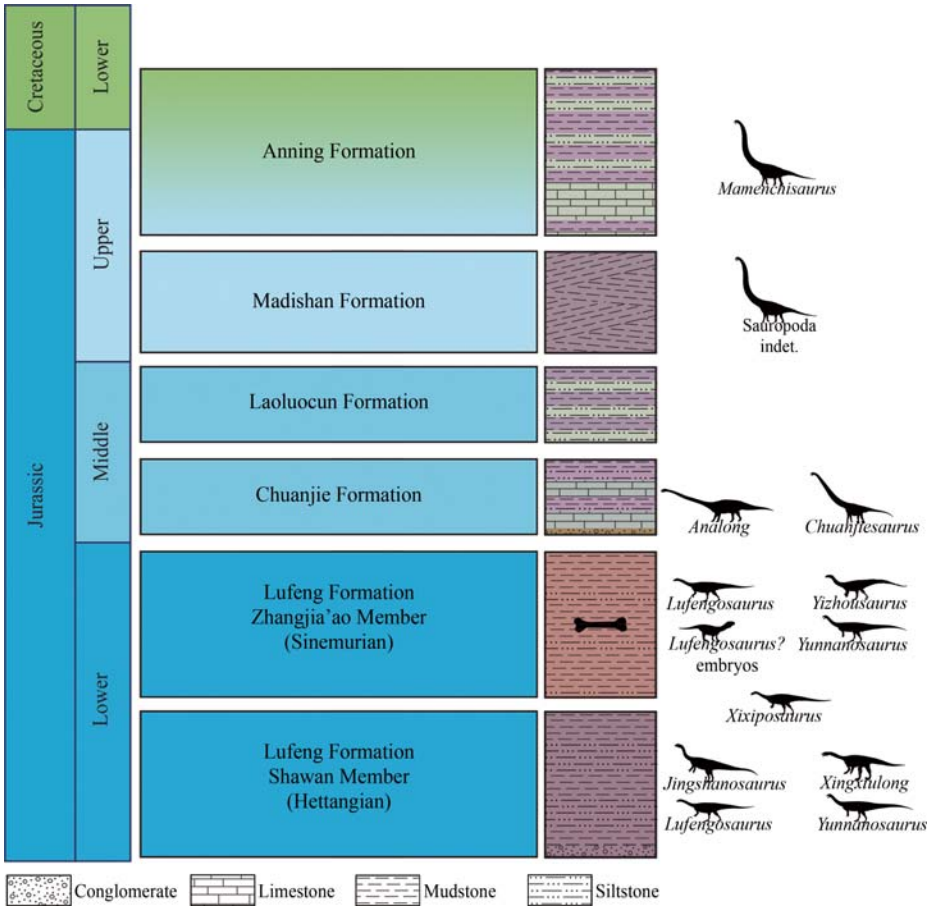

Fig. 2. Chrono-biostratigraphy and lithology of the Mesozoic 'Red Beds' of Yunnan, with the location of new fossil CVEB22001.

Lithology major components: interbedded (horizontal pattern), or cross-bedded (diagonal pattern). Solely sauropodomorph genera based on body fossils displayed. NB. *Xixiposaurus* (see Table 1) cannot be placed as its exact horizon within the Lufeng Fm. is unknown.

Fang et al., 2008). The Shawan Member has two type sections: one at Shawan, and one at Dahuangtian. The Zhangjia'ao Member has one type section between Shawan and Dahuangtian (Fang et al., 2000: see fig. 1). The Shawan Member is dated as Hettangian, and the Zhangjia'ao Member is commonly considered to be Sinemurian in age (Luo and Wu, 1994; Reisz et al., 2013: fig. 2).

2.2. Lufeng Paleontology

Notably, the Lufeng Fm. sediments are the richest Mesozoic unit of Yunnan Province for many terrestrial tetrapods, and one of the best records for that time worldwide (Young, 1940; Sun et al., 1985; Luo and Wu, 1994). The Lufeng Fm. has yielded amphibians, chelonians, crocodylomorphs, cynodonts, dinosaurs, lepidosaurs and mammals, among others (Young, 1951; Simmons, 1965; Luo and Wu, 1994). The dinosaur and mammal faunas from the Lufeng Fm. are considered equivalent to those of the upper Elliot Fm. in South Africa and the Trossingen Fm. in Germany (Luo and Wu, 1995; Reisz et al., 2013). A variety of invertebrate fossils have also been described from the Lufeng Fm. Most are ostracods, but bivalves and gastropods have also been reported (Simmons, 1965; Fang et al., 2008).

Over time, more than 100 non-sauropodan sauropodomorph specimens have been excavated from the Lufeng Fm., among which a good number were reported in past faunal reviews (Young, 1951; Sun et al., 1985; Fang et al., 2000; Mao et al., 2019). The basalmost unit, the Shawan Member, has yielded four genera and six different species of non-sauropodan sauropodomorphs (Fig. 2; Table 1). Here, we choose not to include *Chuxiongosaurus lufengensis*, as we concur with Zhang et al. (2019) regarding its synonymy with *Jingshanosaurus xinwaensis*. Immature specimens have not been reported from the Shawan Member. The sauropodomorph fauna of the Zhangjia'ao Member, where the specimen described herein was found, includes four genera and five species (Fang et al., 2000) (Fig. 2; Table 1). From the same horizon, only a deformed juvenile specimen, referred to *Lufengosaurus huenei* (Sekiya and Dong, 2010), is known. Surprisingly, sauropodomorph tracks have never been reported from either member of the Lufeng Fm.

The Middle Jurassic Chuanjie Fm. has yielded two sauropod specimens attributed to the mamenchisaurid

Table 1 List of valid sauropodomorph taxa found in the Lufeng fauna, Lufeng County, Yunnan

	Material (holotype no)	Type locality	Institution	Completeness (%)
Analong chuanjieensis (Ren et al., 2020)	1 specimen (LCD9701-I)	A'na village	Lufeng World Dinosaur Valley Yunnan (LWDV)	50
Chuanjiesaurus anaensis (Fang et al., 2000)	1 specimen (Lfch 1001)	Laochangqing village	LWDV	32
Jingshanosaurus xinwaensis (Zhang and Yang, 1995)	2 specimens (LFGT-ZLJ0113)	Xinwa village	LWDV	95
Lufengosaurus huenei (Young, 1941)	≈90 specimens (IVPP V15)	Shawan village	Institute of Vertebrate Paleontology and Paleoanthropology, Beijing (IVPP)	100
Lufengosaurus magnus (Young, 1947)	19 specimens (IVPP V82)	Tachung village	IVPP	73
Mamenchisaurus yunnanensis (Fang et al., 2004)	1 specimen (V1481)	Between Laochangqing & Dajianfeng villages	The Geological Museum of China, Beijing	13
Xingxiulong chengi (Wang et al., 2017)	3 specimens (LFGT-D0002)	Sakenshu village	LWDV	77
Xixiposaurus suni (Sekiya, 2010)	1 specimen (ZLJ0108)	Xixipo village	LWDV	55
Yizhousaurus sunae (Zhang et al., 2018)	1 specimen (LFGT-ZLJ0033)	Duwafang village	LWDV	82
Yunnanosaurus huangi (Young, 1942)	13 specimens (NGMJ 004546)	Huangjiatian* village	IVPP	68
Yunnanosaurus robustus (Young, 1951)	7 specimens (IVPP V93)	Huangjiatian* village	IVPP	59

Total number of specimens includes only those excavated from the "Lufeng Group". Completeness is estimated based on material known from holotype and referred specimens. Institutional abbreviations: Lfch = Lufeng Museum; LFGT = Bureau of Land and Resources of Lufeng County; NGMJ = Nanjing Geological Museum; ZLJ = Lufeng World Dinosaur Valley. *Originally spelled Huangchiatien by Young, using an old romanization system of mandarin Chinese.

Chuanjiesaurus (Fang et al., 2000; Sekiya, 2011). Recent re-examination of the material led to the creation of a new mamenchisaurid taxon named *Analong* (Ren et al., 2020) (Fig. 2; Table 1). The Chuanjie Fm. has also produced sauropod tracks attributed to mamenchisaurids (Xing et al., 2014).

The Upper Jurassic Madishan Fm. record is scarce with only indeterminate sauropod bones (Fang et al., 2008: fig. 2).

Finally, strata of the Upper Jurassic Anning Fm. yielded a new species of *Mamenchisaurus* (Fang et al., 2004) (Fig. 2; Table 1). This attribution was recently questioned, some authors claiming that the material recovered in Yunnan is too fragmentary and, basically, undiagnostic (Ye, 2008; Wang et al., 2019).

3 Material and Methods

The specimen CVEB22001 consists of a partial right skull, one complete and four partial anterior cervical vertebrae, one complete and two partial middle to posterior dorsal vertebrae, two complete right metacarpals, the distal end of the right femur and the proximal end of the right tibia. The material is housed in the Centre for Vertebrate Evolutionary Biology, Yunnan University, Kunming (CVEB). It was mechanically prepared using pin vices and other hand tools, as well as air scribes.

Osteohistological sections were produced at Yunnan University. The femur diaphysis was sectioned using a diamond saw, and the thin transverse section was generated in accordance with the following procedure: the broken proximal surface of the femur was leveled and polished on a grinding wheel with increasingly fine carborundum grades (120, 400 and 800). Subsequently, the resulting polished surface was attached to a microscope slide with resin and hardener, EpoThin epoxy, and ground to approximately 30 μm in thickness.

Optical examination and rendering were carried out under normal light using a Zeiss microscope Imager A2 equipped with a digital camera (Zeiss Axiocam ICc5), and under polarized light using a Zeiss polarizing microscope Axio Imager.M2m equipped with a digital camera (Zeiss Axiocam 506 color). Image capture was carried out using a Leica LAS 4.10 and ZEN (Zeiss) microscope software under normal light, as well as ZEN core 2.6 (Zeiss) under polarized light.

3.1 Phylogenetic analysis

The phylogenetic relationships of CVEB22001 were inferred based on the dataset of Zhang et al. (2019), including 61 taxa and 364 characters. Following the original authors, 43 multistate characters were considered additive (8, 13, 19, 23, 40, 57, 69, 92, 102, 117, 121, 131, 134, 145, 148, 150, 151, 158, 163, 168, 171, 178, 185, 208, 211, 218, 226, 231, 238, 246, 254, 257, 270, 282, 303, 309, 317, 337, 350, 353, 355, 360, 364). A total of 48 characters, 13% of the total number (supplementary S1), were scored on the skull, vertebrae, forelimb and hindlimb. For those 48 characters, the scoring was checked for all taxonomic units, with a particular attention to Chinese taxa, and modifications were made in nine characters (supplementary S2).

The phylogenetic analysis was run using TNT version 1.5 (Goloboff and Catalano, 2016). The traditional search method was employed, with 1000 replicates of additional sequences and a tree bisection reconnection (TBR) swapping algorithm with 10 trees per replication. The analysis resulted in 10 most parsimonious trees, each

with a length of 1291 steps, a consistency index of 0.33 and a retention index of 0.69. Figure 7 displays the simplified strict consensus tree of these 10 most parsimonious trees showing only a selected sample including the earliest sauropodomorphs and taxa with close affinities with the described specimen CVEB22001.

4 Systematic Paleontology

Super-order Dinosauria Owen, 1842
Order Saurischia Seeley, 1887
Sub-order Sauropodomorpha von Huene, 1932
Clade Massopoda Yates, 2007
Massopoda gen. et sp. indet.

Description and comparisons are provided below.

4.1 Skull ~ Antorbital fenestra and fossa

The antorbital fenestra is not entirely preserved, only its ventral margin is visible (Fig. 3). Usually in non-sauropodan sauropodomorphs, it is a subtriangular opening posterior to the naris. In CVEB22001, the ventral margin of the fenestra is particularly extended at circa twice the length of the lacrimal base. It is reminiscent of that seen in the juvenile *Massospondylus* (Sues et al., 2004; Chapelle et al., 2019).

In the anteroventral corner of the antorbital fenestra, the antorbital fossa is thin with a sharp margin. Posteroventrally, the extension of the antorbital fossa on the lacrimal is absent, as in the juvenile *Yunnanosaurus robustus* (Sekiya et al., 2014). It has been observed that it is shallower in non-adults than in adults (Sues et al., 2004), although it is still present in the juvenile *Massospondylus*. The extension of the fossa on the lacrimal is also observed in adults *Lufengosaurus* (Barrett et al., 2005) and *Yizhousaurus* (Zhang et al., 2018).

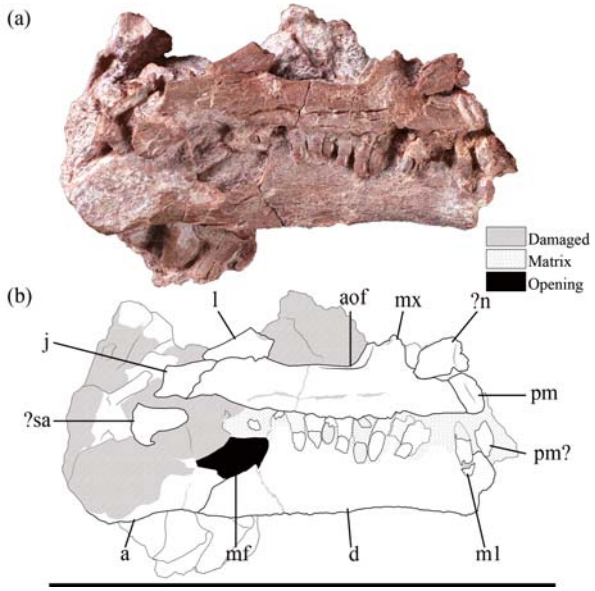

Fig. 3. Photograph (a) and interpretative drawing (b) of the right side of the skull of CVEB22001.
Scale bar = 10 cm.

4.2 Skull ~ Premaxilla

The premaxilla is a short bone forming the tip of the snout. It is very incomplete in CVEB22001, with only a small rectangular fragment preserved in articulation with the maxilla (Fig. 3). At the contact point between the posterior premaxillary margin and the anterior maxillary margin, the subnarial foramen is not visible. One tooth, presumably the last premaxillary tooth, is preserved ventral to the premaxilla fragment.

4.3 Skull ~ Maxilla

The maxilla is a triradiate bone forming the posterior and ventral margins of the naris and the ventral and anterior margins of the antorbital fenestra. The right maxilla in CVEB22001 is nearly complete, lacking only the nasal process, and is 52 mm long (Fig. 3).

The lateral surface of the maxilla is flat and does not exhibit any obvious neurovascular foramen. This is surprising given that most Jurassic non-sauropodan sauropodomorphs in which the maxilla is known, have a row of neurovascular foramina on it. The only species to show a complete absence of foramina is the adult form of *Yunnanosaurus huangi* (Barrett et al., 2007).

The premaxillary ramus of the maxilla is low and elongate prior to the nasal process, as in juveniles of *Mussaurus* (Pol and Powell, 2007) and *Yunnanosaurus robustus* (Sekiya et al., 2014), and adult or subadult forms of *Jingshanosaurus* (Zhang and Yang, 1995; Zhang et al., 2019), *Lufengosaurus huenei* (Barrett et al., 2005), *Xixiposaurus* (Sekiya, 2010) and *Yimenosaurus* (Bai et al., 1990).

On the dorsal margin of the maxilla, the thin base of the nasal process projects dorsally. Its posterior margin is cleft by a deep groove, the antorbital fossa, extending along the dorsal margin of the maxilla jugal ramus. Conversely to the condition observed in several adult forms, the antorbital fossa does not have a significant extension on the maxilla, either anterior as in the adult *Lufengosaurus huenei* (Barrett et al., 2005), or ventral as in *Yizhousaurus* (Zhang et al., 2018) and *Yunnanosaurus huangi* (Barrett et al., 2007).

Along the maxillary tooth row, some alveoli show replacement teeth in situ, and ten erupted teeth are preserved. The teeth are abutted against the dentary, and, therefore, only their labial surfaces are exposed. They look robust, but are all damaged to some extent. All the maxillary teeth bear denticles on both carinae.

4.4 Skull ~ Lacrimal

Only the ventral part of the lacrimal is preserved in CVEB22001 (Fig. 3). It slopes strongly anterodorsally, in contrast with the adult *Yizhousaurus* (Zhang et al., 2018), and expands anteroposteriorly towards the ventral end of the bone. The lacrimal lateral surface is gently concave, whereas the flat medial surface is divided into two subequal surfaces by a low median ridge. The ventral end of the bone contacts the maxilla anteriorly and the jugal posteriorly.

4.5 Skull ~ Jugal

Only the anterior process of the bone is preserved (Fig.

3). It tapers towards the anterior subtriangular end. The jugal does not contribute to the antorbital fenestra, unlike in the adult *Yizhousaurus* (Zhang et al., 2018).

4.6 Skull ~ Dentary

The dentary is a straight bone forming the most important part of the mandible. The CVEB22001 right dentary is nearly complete, but its anterior end is broken off (Fig. 3). The dentary is stuck behind the upper jaw, so that its dorsal margin is not exposed. The ventral and dorsal margins of the dentary are subparallel on the anterior part of the bone and move apart progressively posteriorly, so that the maximum height of the bone is at the posterior end. In contrast, the maximum width of the dentary occurs at its anteriormost part.

The lateral surface of the dentary is gently concave anteroposteriorly and does not exhibit any row of foramina, as in the juvenile *Arcusaurus* (Yates et al., 2011). The dentary ridge, present in the adult form of *Lufengosaurus huenei* (Barrett et al., 2005), is absent, as well as the lateral convexity observed in the juvenile *Yunnanosaurus robustus* (Sekiya et al., 2014).

The posterior margin of the dentary is divided into two slender processes and forms the anterior margin of the external mandibular fenestra. The posteroventral process of the dentary sutures with the angular. It is subtriangular and laterally overlaps the angular.

4.7 Skull ~ Dentition

Along the ventral margin of the maxilla, ten erupted teeth are preserved (Fig. 3). They are linearly placed, as in both adult and juvenile *Yunnanosaurus* (Barrett et al., 2007; Sekiya et al., 2014). The teeth are straight, labiolingually compressed, and folidont with a reniform cross-section (Hendrickx et al., 2015). The crown is spatulate, with a convex labial surface and a mildly concave lingual surface. The mesiodistally widest point of the crown is located at its base, as in most non-sauropodan sauropodomorphs (Galton and Upchurch, 2004).

The maxillary dentition is heterodont: the anteriormost maxillary crown is 8 mm long; the posteriormost is 4 mm. The same degree of heterodonty is observed in both juvenile and adult *Massospondylus* (Sues et al., 2004: fig. 8) and in juvenile *Yunnanosaurus robustus* (Sekiya et al., 2014: fig. 2).

The carinae bear small denticles, a condition observed in most non-sauropodan sauropodomorphs except for adult *Yunnanosaurus huangi* (Barrett et al., 2007) and *Irisosaurus yimenensis* (Peyre de Fabrègues et al., 2020). There are five denticles on each carina, which is less numerous than in the juveniles *Arcusaurus* (Yates et al., 2011) and *Mussaurus* (Pol and Powell, 2007). At the apex of the crown, no wear facets such as those reported in juvenile *Yunnanosaurus robustus* (Sekiya et al., 2014) are visible.

The tooth enamel is mostly smooth, as in adults *Lufengosaurus* (Barrett et al., 2005), *Xixiposaurus* (Sekiya, 2010), *Yizhousaurus* (Zhang et al., 2018) and *Yunnanosaurus* (Barrett et al., 2007; pers. obs., ZLJ0110).

4.8 Vertebrae ~ Cervical vertebrae

One complete and four partial anterior cervical vertebrae are preserved in CVEB22001 (Figs. 4a–b; Table 2). The cervical vertebrae are elongated, with no

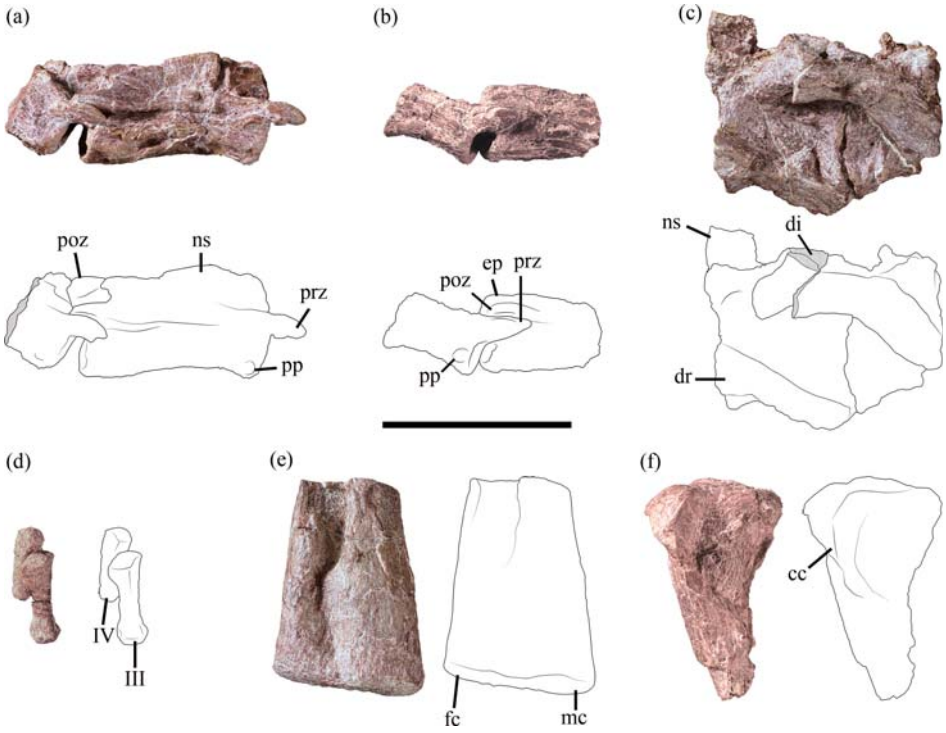

Fig. 4. Photographs and interpretative drawings of the postcranial elements of CVEB22001.
(a–b) Anterior cervical vertebrae in right lateral view; (c) middle to posterior dorsal vertebrae in left lateral view; (d) right metacarpals in dorsal view; (e) right femur in anterior view; (f) right tibia in anterior view. Abbreviations: cc = cnemial crest; dr = dorsal rib; ep = epipophysis; fc = fibular condyle; mc = medial condyle; ns = neural spine; poz = postzygapophysis; pp = parapophysis; prz = prezygapophysis; IV & III, metacarpals IV & III; Scale bar = 5 cm.

Table 2 Measurements (mm) of the vertebrae of CVEB 22001

	L	antW	postW	antH	postH	nsH	nsL	H
Cant	47	16	18*	16	13*	9	45	31
Cant	?	15*	?	19*	?	?	?	?
Cant	?	?	16	?	?	?	?	?
Cant	?	14	?	15	?	?	?	?
Dmid-post	34	24	?	22	28	?	?	?
Dmid-post	?	?	?	28	?	?	?	?

antH = centrum anterior height; antW = centrum anterior width; Cant = anterior cervical vertebra; Dmid-post = middle to posterior dorsal vertebra; H = total height of the vertebra; L = maximum anteroposterior ventral length; nsH = maximum neural spine height; nsL = maximum neural spine length; postH = centrum posterior height; postW = centrum posterior width; * = deformation.

marked pneumatization. The complete anterior cervical vertebra is 47 mm long, with a length over height ratio of 2.94. This is close to the ratio of the juvenile *Lufengosaurus huenei* (3.21 on 4th cervical vertebra; Sekiya and Dong, 2010), and higher than that of juveniles *Mussaurus* (1.69; Otero et al., 2019) and *Yunnanosaurus robustus* (1.45; Sekiya et al., 2014). Cervical centra exhibit amphicoelous and circular articular surfaces and, in ventral aspect, a marked median constriction. None of the centra bears a ventral ridge.

Parapophyses are reduced in size, low and located in the anteroventral corner of centra. Some are still in articulation with the proximal end of the cervical rib.

Diapophyses are also low, incipient, and do not project.

Prezygapophyses are long, although not mounted on pedicels. Their articular surfaces are flat, oval-shaped in outline and facing dorsomedially.

Postzygapophyses project posteriorly and exhibit a flat, ventrally to ventrolaterally oriented articular surface. The dorsal surface of all the postzygapophyses bears a well-defined and elongated epipophysis. Epipophyses are low and merged with postzygapophyses throughout their length. In contrast, postzygapophyses on anterior cervical vertebrae of the juvenile *Plateosaurus engelhardti* do not bear an epipophysis (Hofmann and Sander, 2014).

Below the neural spine, the cervical neural arch is low. The neural spine is long and transversely compressed. In lateral aspect, the dorsal margin of the neural spine is gently convex, and the posterodorsal corner projects posteriorly.

4.9 Vertebrae ~ Dorsal vertebrae

One complete and two partial middle to posterior dorsal vertebrae are preserved in articulation (Fig. 4c; Table 2). The dorsal vertebrae are short and high, with no marked pneumatization. The length over height ratio of the complete dorsal vertebra is 1.55, which is higher than that of the juvenile *Yunnanosaurus robustus* (1.44 and 0.89 for middle and posterior dorsal vertebra, respectively; Sekiya et al., 2014). Dorsal centra have oval articular surfaces, with a dorsoventral long axis. In ventral aspect, centra exhibit a median constriction but no ventral ridge.

Parapophyses are subcircular and located on the neural arch, anteroventrally to the diapophysis. On this basis, we postulate that vertebrae are posterior to D8. The same disposition is observed in the juvenile *Plateosaurus engelhardti* (Hofmann and Sander, 2014). Parapophyses are low, and one of them is still in articulation with the articular facet of a dorsal rib.

The preserved diapophysis is flat, subrectangular in outline, and projects dorsolaterally. At the distal end of the diapophysis, the articular facet for the rib is oval in outline.

Postzygapophyses are hardly visible, and project further posteriorly than the posterior margin of the dorsal centrum.

The neural arch is lower than in posterior dorsal vertebrae of the juvenile *Ignavusaurus* (Knoll, 2010). Below the neural spine, the neural arch height represents approximately half of the centrum height. The neural spine is anteroposteriorly longer than transversely wide. In lateral aspect, the dorsal margin of the neural spine is straight, with no projecting posterodorsal corner.

4.10 Forelimb ~ Metacarpals

Two complete right metacarpals were preserved in articulation (Fig. 4d; Table 3). Based on their shape and articulation pattern, they are identified as metacarpals III and IV. Their size is close to that of metacarpals III and IV of the juvenile *Ignavusaurus* (25 and 19 mm, and 22 and 17 mm, respectively).

Metacarpal III is elongated and gracile, with proximodistally concave medial and lateral surfaces. The distal end of metacarpal III is trapezoidal in outline and bears a shallow collateral fossa on each distal condyle. The proximal end of metacarpal III is more extended transversely than the distal end, like in most non-sauropodan sauropodomorphs. It is subrectangular in outline, with a dorsoventral long axis. The articular facet for metacarpal IV is situated on the ventrolateral surface of metacarpal III.

Metacarpal IV is shorter than metacarpal III, with a proximodistally concave medial margin and a straight lateral margin. The proximal end is clearly wider transversely than the distal one. The distal end of metacarpal IV is subcircular in outline, whereas the proximal end is subtriangular. Metacarpal IV has been moved proximally relative to its in vivo position so that almost all the medial area of the bone, instead of just the proximomedial corner, is in contact with metacarpal III.

4.11 Hindlimb ~ Femur

The distal end of the CVEB22001 right femur is preserved in articulation with the proximal tibia (Figs. 4e, 5; Table 3). In lateral and medial views, the main axis of the distal femur is rather straight. On the anterior surface,

Table 3 Measurements (mm) of the limb bones of CVEB 22001

	L	proxW	proxT	medW	medT	distW	distT
Metacarpal III (right)	25	9	10	6	4	8	5
Metacarpal IV (right)	19	7	8	5	3	6	6
Femur (right)	?	?	?	?	?	41	36
Tibia (right)	?	30	38	?	?	?	?

L = maximum proximodistal length; T = maximum anteroposterior thickness (without the crest for tibia); W = maximum transverse width.

Fig. 5. Photographs of the articulated femur and tibia of CVEB22001.
Scale bar = 5 cm.

the femur bears a clear extensor groove. On the posterior surface, a deep popliteal fossa is visible between the rounded condyles. This fossa is deeper and transversely narrower than in the juvenile *Yunnanosaurus robustus* (Sekiya et al., 2014). The tibiofibular crest is sharp and well visible. In distal view, the medial condyle is approximately the same size as the lateral and fibular condyles put together, even though the fibular condyle is less massive, with a lower transverse width. The distal end of the femur is quadrangular in outline, with a transverse width slightly superior to its anteroposterior extension. These proportions differ from those of the juvenile *Yunnanosaurus robustus* (Sekiya et al., 2014), in which the femur distal end is more rectangular.

4.12 Hindlimb ~ Tibia

The proximal end of the right tibia is preserved in articulation with the distal femur (Figs. 4f, 5; Table 3). The proximal end of the tibia exhibits a cnemial crest and two condyles, as in all non-sauropodan sauropodomorphs. In anterior aspect, the lateral condyle projects slightly more dorsally than the medial condyle. The proximal articular surface is flat and, without considering the cnemial crest, suboval in outline. This shape differs from the circular one of the juvenile *Yunnanosaurus robustus* (Sekiya et al., 2014) and the subtriangular one of an indeterminate juvenile sauropodomorph from the Triassic of Brazil (Pretto et al., 2016).

The cnemial crest is oriented anterolaterally, and its dorsalmost point is located on its proximal end as seen in lateral view. The proximal part of the cnemial crest is sharp, which differs from the blunt crest of the juvenile *Yunnanosaurus robustus* (Sekiya et al., 2014). An elongate depression, visible in medial view, is located between the cnemial crest and the rest of the tibia. The lateral surface of the bone bears another depression, although shallower, separating the cnemial crest from the lateral condyle. An intercondylar groove is not present, in contrast with *Ignavusaurus* (Knoll, 2010).

5 Discussion

5.1 Ontogenetic stage and osteohistology

In dinosaurs, adult or non-adult status is usually detected based on a set of attributes including body size, osteological fusion, bone surface texture, and osteohistology (Sampson et al., 1997; Hone et al., 2016; Table 4). Among non-adult specimens from Jurassic localities, *Ignavusaurus* (Knoll, 2010) has been histologically aged at 1 year old or less, while the exact ontogenetic stages of *Arcusaurus*, *Lufengosaurus*, *Massospondylus* and *Yunnanosaurus* have not been investigated further, they were merely described as juveniles (Sekiya and Dong, 2010; Gow et al., 1990; Sekiya et al., 2014).

Ontogenetically, most of the skeletal remains of CVEB22001 bear no indications of juvenile status. CVEB22001 is small, within the range of early sauropodomorph juveniles. Nonetheless, other key criteria suggesting non-adult status, including size of the orbits or fusion of parietals, cannot be ascertained. The vertebrae seem to have closed neurocentral sutures, but it is not possible to judge the exact degree of osteological fusion in the light of the poor preservation and scarce vertebral material. In the same vein, the bone surface texture on the articular ends of the femur and tibia is mildly rugose. Thus, cursory examination of the material does not make a strong case for non-adult status, although several observations (size, texture) point in that direction.

In order to address the question of the ontogenetic stage of CVEB22001, we examined the bone microstructure. An

Table 4 Comparison of criteria to assess ontogenetic status in immature sauropodomorph specimens excluding embryos (from Hone et al., 2016)

Taxon	Original publication	Specimen	BD	OF	RBT	EM	DS	LAG
A. pereirabdalorum	Yates et al., 2011	BP/1/6235	?	No	?	No	NA	?
E. minor	Galton and Bakker, 1985	SMNS 12667	?	No	?	?	NA	?
P. caducus	Galton et al., 2007	NHMUK RU P24	0.7 m	No	No	No	NA	?
Thecodontosaurus sp.	Benton et al., 2000	?	1.0 m	No	No	No	NA	?
M. carinatus	Gow et al., 1990	BP/1/5253	1.2 m	?	?	No	NA	Yes
M. patagonicus	Pol and Powell, 2007	MPM 1813/10	1.2 m	?	No	No	NA	No
E. browni	Durand, 2001	?	1.5 m	?	?	No	NA	?
I. rachelis	Knoll, 2010	BM HR 20	1.5 m	No	No	No	NA	No
Massopoda indet.		CVEB22001	1.7 m	?	No	No	NA	No
Y. robustus	Sekiya et al., 2014	ZMNH-M8739	4.3 m	No	No	No	NA	?
L. huenei	Sekiya and Dong, 2010	ZLJ0112	5.5 m	No	?	No	NA	?

Specimens are sorted according to estimated body size. BD: estimated body size; EM: eggs or medullary bone associated with the material; DS: display structures (e.g., frills, horns); LAG: Presence of LAGs in osteohistological thin sections; OF: osteological fusion (in skull, scapulocoracoid or vertebrae); RBT: rugose bone texture (limb bone articular surfaces exhibiting well-developed pits and grooves). Institutional abbreviations: BM = Lesotho National Museum in Maseru; BP = Evolutionary Studies Institute of Johannesburg (formerly Bernard Price Institute); MPM = Museo Regional Provincial 'Padre M. J. Molina' of Santa Cruz; NHMUK = The Natural History Museum of London; SMNS = Staatliches Museum für Naturkunde in Stuttgart; ZLJ = Lufeng World Dinosaur Valley; ZMNH = Zhejiang Museum of Natural History.

osteohistological section was made of the distal part of the diaphysis in the right femur (Fig. 6). The transverse section shows a broad medullary cavity surrounded by a thin cortex (between 0.9 to 1.3 mm in thickness). The medullary cavity is large and mainly made of cancellous bone, because of the proximity of the section with the epiphysis of the bone. The deformation undergone by the bone is well visible, causing clear recesses and breakages in the cortex (Fig. 6a). The cortical tissue is mainly composed of highly vascularized lamellar bone, and includes many osteocytes associated with large vascular canals. Some canals are visible in transverse section, while some others are in longitudinal section. There is a slight decrease in vascularization towards the outer surface of the cortex (Fig. 6b). Primary osteons are randomly distributed in the cortical bone, and there are no secondary osteons. In high magnification, small and borderless primary osteons appear to have been formed by a large vascular canal surrounded by a few concentric layers of lamellar bone (Fig. 6c). The fact that only a few layers of lamellar bone are built is indicative of an early stage. This observation is supported by the presence of woven bone, the most disorganized bone tissue, also indicative of young age (Fig. 6d). Woven bone is often found in young and growing individuals, as it represents the earliest stage of bone formation (de Ricqlès, 1974; Chinsamy, 1993). Lines of arrested growth (LAGs) and Haversian remodeling are completely absent. It is noteworthy that the outermost areas of the cortex are fairly damaged all around the femur, so superficial structures such as LAGs could be missing. The cortex is nonetheless not entirely eroded, so that only one or two structures, at most, would be absent. This situation, with one LAG in the outmost cortex layer, has already been observed in a small *Massospondylus* (Cerda et al., 2014).

The heavy vascularization of the tissue, presence of woven bone, and absence of LAGs and secondary osteons suggest that CVEB22001 was a juvenile with a fairly fast growth (de Ricqlès, 1974; Chinsamy, 1993). Similar patterns with dense vascularization and primary osteons have been observed in several juvenile non-sauropodan sauropodomorphs, including *Ignavusaurus* (Knoll, 2010), *Massospondylus*, *Mussaurus* (Cerda et al., 2014) and MMACR-PV-028-T (Pretto et al., 2016).

5.2 Comparisons

The osteohistological examination of the femur of CVEB22001 suggests that the specimen is a juvenile, as does the body size. More than 20 young non-sauropodan sauropodomorphs, ranging from perinates to juveniles, are currently known. Worldwide, seven specimens were reported from Lower Jurassic layers, two of which are presently Sauropodomorpha indet. (Young, 1982; Evans and Milner, 1989; Sereno, 1991). The others have been referred to three already existing species: *Lufengosaurus huenei* (Sekiya and Dong, 2010), *Massospondylus carinatus* (Gow et al., 1990; Sues et al., 2004) and *Yunnanosaurus robustus* (Sekiya et al., 2014), and to two other species: *Arcusaurus pereirabdalorum* (Yates et al., 2011) and *Ignavusaurus rachelis* (Knoll, 2010) (Table 4),

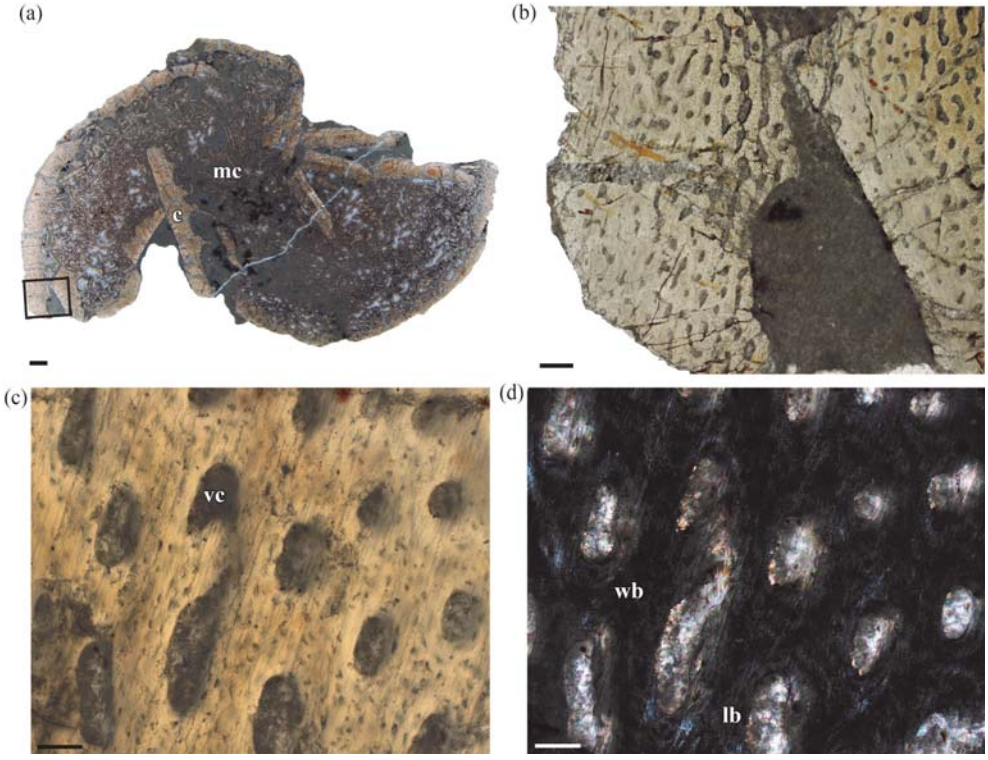

Fig. 6. Osteohistology of the CVEB22001 femur.
General view of the complete cross-section (a) and close-up on the cortical bone, with abundant vascular canals; (b) enlarged view of the cortex showing primary osteons in normal light (c) and same section under polarized light (d).
Abbreviations: c = cortex; lb = lamellar bone; mc = medullary cavity; vc = vascular canals; wb = woven bone. Scale bars = (a) 1 mm, (b) 200 μm, (c) 50 μm, (d) 50 μm.

which are the only instances of isolated immature specimens used to erect a new species. *Ignavusaurus* has been considered to be a junior synonym of *Massospondylus*, whereas demonstration has been made that the *Arcusaurus* material was referable neither to adult *Aardonyx* nor *Massospondylus* (Yates et al., 2011).

Listed below are some key discrepancies between Jurassic juvenile specimens and CVEB22001. In *Arcusaurus pereirabdalorum* (Yates et al., 2011), the dentary exhibits a row of large foramina, and the teeth bear approximately ten denticles on each carina. In *Ignavusaurus rachelis* (Knoll, 2010), dorsal neural arches are tall and there is a well-defined intercondylar notch on the proximal tibia. In *Lufengosaurus huenei* (Sekiya and Dong, 2010), cervical vertebrae bear a ventral ridge. In *Massospondylus carinatus* (Sues et al., 2004; Chapelle et al., 2019), the maxilla posterolateral surface bears a large foramen, the anteroventral corner of the antorbital fossa is large, and the dentary has a constant dorsoventral height throughout its length. In *Yunnanosaurus robustus* (Sekiya et al., 2014), the antorbital fenestra ventral margin and the lacrimal base have a similar anteroposterior development, the dentary exhibits a lateral convexity, and the tooth crowns bear wear facets.

Estimation of CVEB22001 body size is rather difficult given the incompleteness of the material. Looking at the cranial material, CVEB22001 maxilla (52 mm) is somewhere between juveniles of *Massospondylus* (40 mm) and *Yunnanosaurus* (70 mm). Regarding postcrania, we used data collected from the femora of 25 early sauropodomorphs to calculate the mean ratio of the femoral total length over distal transverse width. Both adults and juveniles were included in the sample, since the point was made that sauropodomorph femora developed isometrically (Kilbourne and Makovicky, 2010). The mean ratio obtained was 4. On this basis, we suggest an estimated femoral length of 170 mm for CVEB22001. Hence, CVEB22001 is somewhat larger than *Ignavusaurus* (femur: 154 mm), but considerably smaller than *Lufengosaurus* (femur: 550 mm) and *Yunnanosaurus* (femur: 435 mm) juveniles. Measurements and comparisons on both the maxilla and femur are consistent, showing that CVEB22001 is of intermediate size (Table 4). Based on the estimated femoral length, and assuming that both taxa had roughly the same growth rate, the model presented by Chinsamy (1993: fig. 7) for *Massospondylus* indicates that CVEB22001 could possibly be between 3 and 4 years old.

Anatomical and size comparisons with immature specimens from the Lower Jurassic do not bring to light strong affinities with any particular species. More importantly, the most likely closely related/similar juveniles (i.e., *L. huenei* and *Y. robustus*) are only known from incomplete skeletons, and the referrals of these immature specimens to *Lufengosaurus* and *Yunnanosaurus* lack a strong anatomical basis (S4). In that respect, it is important to consider the possibility that CVEB22001 might represent an early ontogenetic stage of the coeval *Lufengosaurus*, *Yizhousaurus* or *Yunnanosaurus* (Fig. 2). To address this last point, a review of the diagnostic characters of these three taxa, along with key discrepancies with CVEB22001, is proposed hereafter.

The adult *Lufengosaurus huenei* (Young, 1940; Barrett et al., 2005) has one diagnostic character on the maxilla that is not observed in CVEB22001: presence of a ridge on posterior part of lateral surface (Fig. 3). Four non-diagnostic characters are also not observed in CVEB22001: important extension of the antorbital fossa on the maxilla, presence of a ridge on lateral surface of the dentary, maxillary teeth in en-echelon arrangement, and presence of a ventral ridge on cervical centra.

The adult *Yizhousaurus sunae* (Zhang et al., 2018) has three diagnostic characters located on the skull and mandible, which are not observed in CVEB22001: lateral plates appressed to the labial sides of the premaxillary and maxillary teeth, lacrimal shaft vertical with respect to the maxillary ramus, and tiny external mandibular fenestra (Fig. 3). Three non-diagnostic characters are also not observed in CVEB22001: important extension of the antorbital fossa on the maxilla, extension of the antorbital fossa on the lacrimal, presence of a ventral ridge on cervical centra.

The adult *Yunnanosaurus huangi* (Young, 1942; Barrett et al., 2007) has two cranial diagnostic features not found in CVEB22001: shallow, subcircular fossa present on lateral surface of ventral lacrimal process, and maxillary teeth mesiodistally narrow and lacking denticles (Fig. 3). Two non-diagnostic features are also not found in CVEB22001: important extension of the antorbital fossa on the maxilla, and antorbital fossa delimited by a low, rounded rim on the ascending ramus of the maxilla.

The adult *Yunnanosaurus robustus* (Young, 1951) cannot be compared with CVEB22001 based on diagnostic features (defined on astragalus and metatarsal IV by Sekiya et al., 2014) because no elements overlap. However, three non-diagnostic features are not observed in CVEB22001: presence of large foramina on the anterior ramus of the maxilla, dentary with a constant dorsoventral height throughout its length, and relatively short cervical vertebrae with tall neural arches.

In this context, a taxonomic assignment of CVEB22001 is challenging for multiple reasons: the incompleteness of the material at hand, the lack of comparative material of equivalent ontogenetic stage and the fact that anatomical comparisons between adult and juvenile specimens can prove to be tricky, because many of CVEB22001 morphological characters are still likely to undergo ontogenetic changes. This last matter can be dealt with by discussing maturity-dependent characters.

5.3 Phylogenetic affinities and maturity-dependent characters

The phylogenetic analysis recovers CVEB22001 as a member of the Massopoda (Fig. 7). It is located crownward to Plateosauridae and Massospondylidae, but in an earlier-branching position than Sauropodiformes. CVEB22001 is found in a polytomy including *Eucnemesaurus*, *Riojasaurus* and the clade *Seitaad* + Sauropodiformes. The phylogenetic analysis does not reveal close affinities with any Lufeng taxon. Relative to Chinese coeval taxa, CVEB22001 is recovered crownward

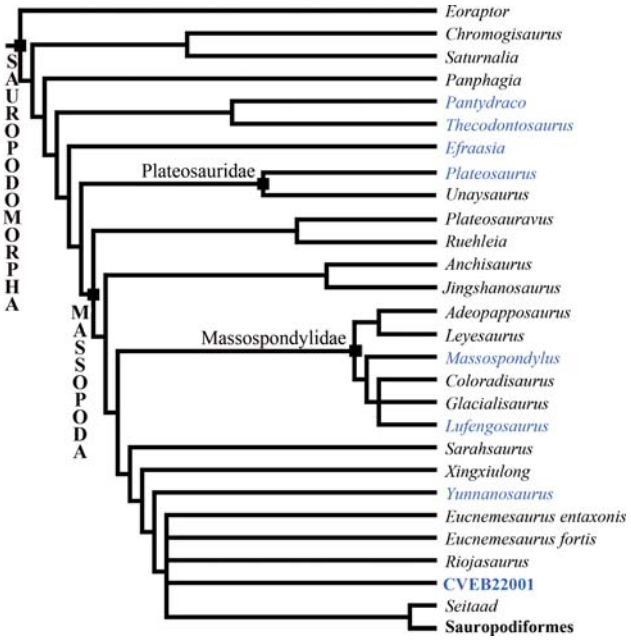

Fig. 7. Simplified strict consensus tree of 10 most parsimonious trees produced by the analysis of a matrix modified from Zhang et al. (2019) showing phylogenetic relationships of CVEB22001 within the Sauropodomorpha. Colored taxa are those for which one or several juvenile specimens have been reported. CVEB22001 and *Pantydraco* are the only taxonomic units known solely from immature specimens.

to *Lufengosaurus* and *Yunnanosaurus*, but stemward to *Yizhousaurus*.

We note that, when dealing with immature specimens, phylogenetic affinities should be interpreted with great care. Ontogeny generally leads to varying degrees of change in anatomy. It has been underlined that the inclusion of non-adult animals in analyses could result in a taxon being recovered with an incorrect position (Hone et al., 2016). The ontogeny of *Lufengosaurus huenei*, in particular, has already been discussed and several discrepancies between juvenile and adult forms underscored: shape of neurovascular foramina; frontal contribution to the dorsal margin of the orbit and to the supratemporal fossa; visibility of the supratemporal fenestra; inclination of the supraoccipital; position of the parasphenoid rostrum; length of the retroarticular process; and projection of the axial postzygapophyses (Sekiya and Dong, 2010). Most of these characters are maturity-dependent and should therefore be avoided when conducting comparisons between a juvenile and an adult form. In datasets, maturity-dependent characters include mainly characters linked to fusion or co-ossification and muscle attachment structures. Fusion or co-ossification are primarily witnessed in skull elements (fusion of parietals) or vertebrae (fusion of centrum and neural arch), but can also be observed on the pectoral girdle (fusion of scapula and coracoid), pelvis elements (fusion of ilium and pubis) and ankle (fusion of astragalus and calcaneum). Muscle attachment structures refer to development of fossae, for instance, as well as trochanters on the femur and humerus (Tykoski, 2005; Yates et al., 2011).

A number of differences between CVEB22001 and adult forms found in the same horizon are pointed out above. As demonstrated below, some of these morphological characters are not maturity-dependent features.

Important extension of the antorbital fossa on the maxilla (versus modest extension in CVEB22001). Adult forms of *Lufengosaurus huenei*, *Yizhousaurus sunae* and *Yunnanosaurus huangi* show this character state. A juvenile specimen referred to *Massospondylus* (Chapelle et al., 2019: fig. 5B) also bears this feature, as well as the adult *Massospondylus*, in which it is even more developed.

Presence of a ventral ridge on cervical centra (versus absence in CVEB22001). Adult forms of *Lufengosaurus huenei* and *Yizhousaurus sunae* have this feature, as well as a juvenile specimen referred to *Yunnanosaurus robustus* (Sekiya et al., 2014).

Extension of the antorbital fossa on the lacrimal (versus absence of extension in CVEB22001). Adult forms of *Yizhousaurus sunae* and *Yunnanosaurus huangi* show this extension on the ventral part of the lacrimal, as well as a juvenile specimen referred to *Massospondylus* (Chapelle et al., 2019: fig. 5B).

Antorbital fossa delimited by a blunt, rounded rim on the maxilla (versus sharp rim in CVEB22001). This character state is present in the adult form of *Yunnanosaurus huangi*. The other state, a sharp rim, is present in the juvenile specimens referred to *Massospondylus* (Chapelle et al., 2019: fig. 5B) and *Yunnanosaurus robustus* (Sekiya et al., 2014: fig. 2), as well as in the matching adult forms.

Foramina on the anterior ramus of the maxilla (versus absence of foramina in CVEB22001). The adult form of *Yunnanosaurus robustus* shows this feature. It has been pointed out that a juvenile referred to *Massospondylus* shows a cluster of neurovascular foramina on the dentary, just like the adult specimen (Yates et al., 2011).

As a consequence, among the features proposed to distinguish CVEB22001 from other taxa, all of the above seem to be unaffected by maturity. Hence, the hypothesis that CVEB22001 represents an early stage of *Lufengosaurus*, *Yizhousaurus* or *Yunnanosaurus* is rejected.

5.4 Taxonomy

Here we question the attributions of immature specimens to *L. huenei* and *Y. robustus*, beginning with the damaged juvenile specimen ZLJ0112 excavated from the same horizon as CVEB22001 and referred to *L. huenei* by Sekiya and Dong (2010). Our main cause of concern is the inconspicuous character of the diagnostic features on the juvenile specimen, because the authors claimed to observe all the autapomorphies identified on the holotypic skull (Barrett et al., 2005). In fact, most reported autapomorphies are not visible: the low tuberosity on lateral surface of the maxilla ascending process, the low boss on the central portion of the incomplete jugal, and the convexity of the parietal anterolateral process (Sekiya and Dong, 2010: their fig. 2B and C). The maxilla lateral surface bears a slight convexity, identified as homologous

to the autapomorphic ridge. Its position and lack of definition make it hard to identify as such. Moreover, a similar convexity is visible on the anterior part of the dentary, but is not identified as an underdeveloped ridge (Sekiya and Dong, 2010: their fig. 2B). Even though a dentary ridge is observed in adult *Lufengosaurus*, it is located rather posteriorly and dorsally on the bone, near the tooth row (Barrett et al., 2005: their fig. 6). For all these reasons, we do not support the synonymy of ZLJ0112 with *Lufengosaurus huenei*.

The referral of immature material to *Yunnanosaurus robustus* can also be called into question. This species, originally described by Young (1951), was never reviewed since then. The original diagnosis is partly based on the diagnosis, now obsolete, of *Yunnanosaurus huangi* (Young, 1942) and includes features such as "size nearly twice larger than *Yunnanosaurus huangi*" or "Foot is longer stretched in contrast to the extremely short hand". Unable to rely on this original diagnosis, Sekiya et al. (2014) proposed a revised diagnosis including two characters: the absence of anteroposterior expansion on the medial end of astragalus and a dorsoventrally compressed medium shaft of the metatarsal IV. The first character is observed in other sauropodomorph genera, such as *Mussaurus*, while the second character is, to some extent, common.

6 Conclusions

A juvenile specimen, CVEB22001, consisting of a partial right skull and disarticulated postcranial elements is described. It was recovered from the Jurassic (Sinemurian) Lufeng Fm. Zhangjia'ao Member, which has also yielded countless specimens of *Lufengosaurus* and *Yunnanosaurus*. The size of the femur in CVEB22001 is estimated at 170 mm in length, which is less than half that of the juvenile *Lufengosaurus* reported from the same horizon, making CVEB22001 the smallest non-embryonic specimen attested in the Lufeng Fm. Body size, together with bone texture and osteohistological examination of the femur, indicate that CVEB22001 is a juvenile and fast-growing specimen.

Four sauropodomorph species: *Lufengosaurus huenei*, *Yizhousaurus sunae*, *Yunnanosaurus huangi* and *Yunnanosaurus robustus*, are known from several localities near Dahuangtian in the Sinemurian Lufeng Fm. Unfortunately, the CVEB22001 material described here lacks potential autapomorphies and does not allow a genus -level identification. Also, a number of osteological features indicate that CVEB22001 cannot be assigned to coeval taxa, and might instead represent an unknown early sauropodomorph species.

It is noteworthy that many specimens have been collected from the Lufeng Fm., and a large number still await proper study or review. Pending these studies, we do not propose a specific taxonomic assignment for this juvenile Massopoda specimen.

Acknowledgements

Support for this research is from the Double First-Class joint program of Science & Technology Department of Yunnan and Yunnan University (2018FY001-005), the China-Myanmar Joint Laboratory for Ecological and Environmental Conservation, and the National Natural Science Foundation of China (grant number 41688103) to X.X. C.P.D.F. is also funded by the China Postdoctoral Science Foundation. Our sincere thanks to Hongqing Li for assistance on the field, Zhixin Yang for specimen preparation, Xudong Gou for osteohistological section, and Jiawen Liu for thin section photographs. We would like to thank two anonymous reviewers for thorough proofreading and constructive feedback. Susan Turner (Brisbane) assisted with English language.

Manuscript received Jun. 23, 2020
accepted Aug. 30, 2020
associate EIC: FEI Hongcai
edited by Susan TURNER and FANG Xiang

References

Bai, Z., Yang, J., and Wang, G., 1990. *Yimenosaurus*, a new genus of Prosauropoda from Yimen County, Yunnan Province. Yuxiwenbo (Yuxi Culture and Scholarship), 1: 14–23 (in Chinese).

Barrett, P.M., Upchurch, P., and Wang, X.L., 2005. Cranial osteology of *Lufengosaurus huenei* Young (Dinosauria: Prosauropoda) from the Lower Jurassic of Yunnan, People's Republic of China. Journal of Vertebrate Paleontology, 25: 806–822.

Barrett, P.M., Upchurch, P., Zhou, X.D., and Wang, X.L., 2007. The skull of *Yunnanosaurus huangi* Young, 1942 (Dinosauria: Prosauropoda) from the Lower Lufeng Formation (Lower Jurassic) of Yunnan, China. Zoological Journal of the Linnean Society, 150: 319–341.

Benton, M.J., Juul, L., Storrs, G.W., and Galton, P.M., 2000. Anatomy and systematics of the prosauropod dinosaur *Thecodontosaurus antiquus* from the Upper Triassic of southwest England. Journal of Vertebrate Paleontology, 20: 77–108.

Carpenter, K., and McIntosh, J., 1994. Upper Jurassic sauropod babies from the Morrison Formation. In: Carpenter, K., Hirsch, K.F., and Horner, J.R. (eds.), Dinosaur eggs and babies. Cambridge: Cambridge University Press, 265–278.

Cerda, I.A., Pol, D., and Chinsamy, A., 2014. Osteohistological insight into the early stages of growth in *Mussaurus patagonicus* (Dinosauria, Sauropodomorpha). Historical Biology, 26: 110–121.

Chapelle, K.E.J., Barrett, P.M., Botha, J., and Choiniere, J.N., 2019. *Ngwevu intloko*: a new early sauropodomorph dinosaur from the Lower Jurassic Elliot Formation of South Africa and comments on cranial ontogeny in *Massospondylus carinatus*. PeerJ, 7: e7240.

Chinsamy, A., 1993. Bone histology and growth trajectory of the prosauropod dinosaur *Massospondylus carinatus* (Owen). Modern Geology, 18: 319–329.

Dong, Z., 1992. Dinosaurian faunas of China. Beijing: China Ocean Press, 1–188.

Durand, J.F., 2001. The oldest juvenile dinosaurs from Africa. Journal of African Earth Sciences, 33: 597–603.

Evans, S.E., and Milner, A.R., 1989. *Fulengia*, a supposed early lizard reinterpreted as a prosauropod dinosaur. Palaeontology, 32: 223–230.

Fang, X.S., Pang, Q.J., Lu, L.W., Zhang, Z.X., Pan, S.G., Wang, Y.M., Li, X.K., and Cheng, Z.W., 2000. Lower, Middle, and Upper Jurassic subdivision in the Lufeng region, Yunnan Province. In: Editorial Committee of Proceedings of the Third National Stratigraphical Congress of China (eds.), Proceedings of the Third National Stratigraphical Congress of China. Beijing: Geological Publishing House, 208–214.

Fang, X.S., Zhao, X.J., Lu, L.W., and Cheng, Z.W., 2004. Discovery of Late Jurassic *Mamenchisaurus* in Yunnan,